Organic & Biomolecular Chemistry

PAPER

View Article Online
View Journal | View Issue

Cite this: *Org. Biomol. Chem.*, 2014, **12**, 8519

5-Nitroindole oligonucleotides with alkynyl side chains: universal base pairing, triple bond hydration and properties of pyrene "click" adducts†

Sachin A. Ingale,[a] Peter Leonard,[a] Haozhe Yang[a,b] and Frank Seela*[a,b]

Received 14th July 2014,
Accepted 9th September 2014

DOI: 10.1039/c4ob01478b

www.rsc.org/obc

Oligonucleotides with 3-ethynyl-5-nitroindole and 3-octadiynyl-5-nitroindole 2′-deoxyribonucleosides were prepared by solid-phase synthesis. To this end, nucleoside phosphoramidites with clickable side chains were synthesized. The 3-ethynylated 5-nitroindole nucleoside was hydrated during automatized DNA synthesis to 3-acetyl-5-nitroindole 2′-deoxyribonucleoside. Side product formation was circumvented by triisopropylsilyl protection of the ethynyl side chain and was removed with TBAF after oligonucleotide synthesis. All compounds with a clickable 5-nitroindole skeleton show universal base pairing and can be functionalized with almost any azide in any position of the DNA chain. Functionalization of the side chain with 1-azidomethylpyrene afforded click adducts in which the fluorescence was quenched by the 5-nitroindole moieties. However, fluorescence was slightly recovered during duplex formation. Oligonucleotides with a pyrene residue and a long linker arm are stabilized over those with non-functionalized side chains. From the UV red shift of the pyrene residue in oligonucleotides and modelling studies, pyrene intercalation was established for the long linker adduct showing increased duplex stability over those with a short side chain.

Introduction

Early studies on non-discriminatory nucleosides which develop equally strong interactions with the four canonical nucleosides of RNA or DNA were performed with base modified nucleosides such as inosine, 2′-deoxyinosine and analogues thereof as well as sugar modified nucleosides containing canonical bases.[1] However, due to hydrogen bonding, inosine forms a significantly more stable base pair with cytidine than with the other nucleic acid constituents and does not behave strictly as a universal nucleoside.[2] Consequently, other nucleosides showing universal base pairing such as **1**–**4a**[2–4] (Fig. 1) were developed and applied as probes and primers in DNA diagnostics, in synthetic biology and for other purposes.[5,6]

To date, one of the most common universal nucleosides is 5-nitroindole 2′-deoxyribonucleoside (**4a**) developed by Brown and Loakes.[4a] It does not form hydrogen bonds to the canonical nucleosides and "base pairs" are stabilized by stacking interactions.[4] Hybridization of 17-mer oligodeoxyribonucleotide duplexes containing the universal nucleoside **4a** opposite to each of the four natural bases gave T_m-values around 65 to 68 °C which are only 4 to 7 °C lower than the reference duplex.[4a] A 2′-*O*-methylribofuranoside and an acyclic 2′-deoxyribofuranoside of 5-nitroindole have been prepared, and the hydrogen bonding capabilities of DNA duplexes containing the 2′-deoxyfuranosides of 3-carboxamido-5-nitroindole have been investigated.[7] Furthermore, 5-nitroindole nucleoside triphosphates were incorporated in DNA by polymerases and base recognition was studied.[8] This compound has also been used in cycle sequencing with tailed oligonucleotides.[5f] The 7-nitroindole 2′-deoxyribonucleoside was utilized to generate abasic 2′-deoxyribonolactone sites by photochemical glycosylic bond cleavage.[9]

The Huisgen–Meldal–Sharpless azide-alkyne cycloaddition (CuAAC) is a common reaction for the functionalization of DNA as it is bioorthogonal to most other reactions and can be performed under aqueous conditions.[10] To utilize universal nucleosides in the so-called "click" reaction side chains with triple bonds were introduced. Earlier such a study was

[a]*Laboratory of Bioorganic Chemistry and Chemical Biology, Center for Nanotechnology, Heisenbergstrasse 11, 48149 Münster, Germany*
[b]*Laboratorium für Organische und Bioorganische Chemie, Institut für Chemie neuer Materialien, Universität Osnabrück, Barbarastrasse 7, 49069 Osnabrück, Germany. E-mail: Frank.Seela@uni-osnabrueck.de; http://www.seela.net; Fax: +49 (0)25153 406 857; Tel: +49 (0)251 53 406 500*

†Electronic supplementary information (ESI) available: General methods and materials, synthesis, purification, and characterization of oligonucleotides, MALDI-TOF mass spectra, ^{13}C-NMR data, ^{1}H–^{13}C coupling constants, HPLC profiles, fluorescence and UV spectra, and ^{1}H, ^{13}C, DEPT-135, and ^{1}H–^{13}C gated-decoupled NMR spectra. See DOI: 10.1039/c4ob01478b

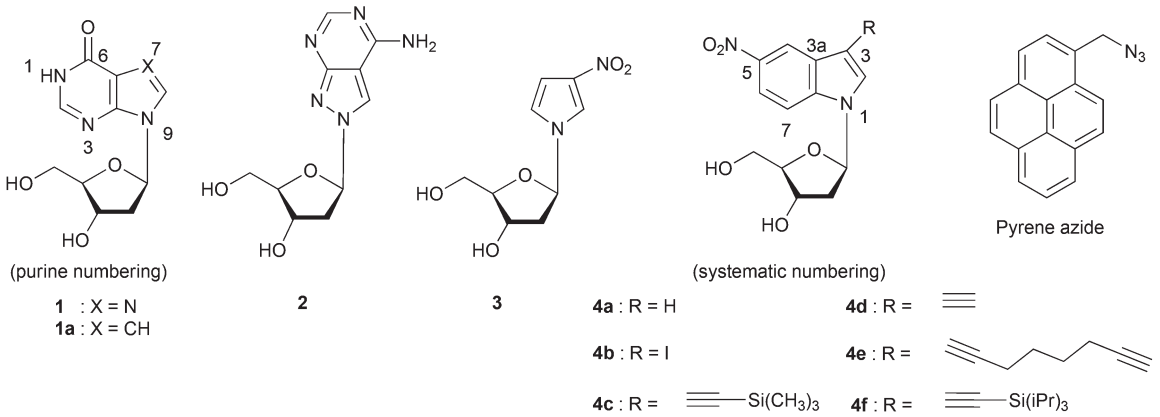

Fig. 1 Structures of universal nucleosides and azide.

performed on the universal nucleoside 7-deaza-2′-deoxyinosine.[11] As 2′-deoxyinosine derivatives do not strictly behave as universal nucleosides, the 5-nitroindole nucleoside **4a** was now chosen. To make compound **4a** applicable for click reactions and click labelling alkynyl side chains were introduced.

This manuscript reports on the synthesis of 3-substituted 5-nitroindole nucleoside phosphoramidites (**10d–f**) derived from the 2′-deoxyribonucleoside **4b** with a iodo substituent, a short side chain **4d** (ethynyl) and a long linker **4e** (octadiynyl) in a sterically non demanding position. The influence of the side chains on the universal base pairing was studied. Also the side chain triple bonds were clicked to the 1-azidomethylpyrene (Fig. 1) applying copper(I) catalyzed CuAAC reaction. The pyrene moiety shows a tendency to intercalate which is expected to be linker dependent. Furthermore, the influence of the dye conjugate on the universal base pairing in duplex DNA and its fluorescence behavior is studied. In case of the ethynyl nucleoside **4d**, by-product formation was observed during oligonucleotide synthesis. The by-product was characterized and its formation was circumvented by triisopropylsilyl protection of the ethynyl function (**4f**).

Results and discussion

Synthesis and characterization of monomers

For the synthesis of nucleosides **4b–f**, the 5-nitroindole base **5** was used as starting material. It was iodinated to give **6** under alkaline conditions (KOH) with iodine (Scheme 1).[5d] Later on, several other reports appeared describing the iodination under various other conditions.[12,13] Similar to the stereoselective nucleobase-anion glycosylation of 4-nitroindole[14a] or 5-nitroindole,[4a] the iodinated nucleobase **6** was treated with 1-chloro-2-deoxy-3,5-di-*O*-(4-toluoyl)-α-D-*erythro*-pentofuranose (**7**),[14b] powdered KOH and TDA-1 (tris[2-(2-methoxyethoxy)ethyl] amine) in acetonitrile under phase-transfer conditions which afforded the protected nucleoside **8**. After removal of inorganic salt, compound **8** was directly crystallized from the crude reaction mixture and was isolated as yellow crystals (90% yield). Deprotection of the toluoyl groups of **8** (7 M methanolic ammonia, 24 h, rt) and precipitation with dichloromethane directly from the reaction mixture furnished nucleoside **4b** in 95% yield as crystalline material. The overall yield (3 steps) calculated on the basis of 5-nitroindole **5** was 83% (Scheme 1). This reaction route was performed without column chromatography and is easily applicable and less hazardous to larger scale as it uses KOH and phase-transfer conditions instead of sodium hydride. A single-crystal X-ray analysis of compound **4b** was performed by our laboratory.[15]

For further functionalization, clickable alkynyl side chains were introduced. To this end ethynyl and octadiynyl residues were installed by the Sonogashira cross-coupling. The reaction was performed on **4b** with trimethylsilylacetylene or octa-1,7-diyne in the presence of CuI/tetrakis(triphenylphosphine)Pd(0) as catalyst (Scheme 2). Following this route, nucleosides **4c** and **4e** containing alkynyl side chains in position-3 were

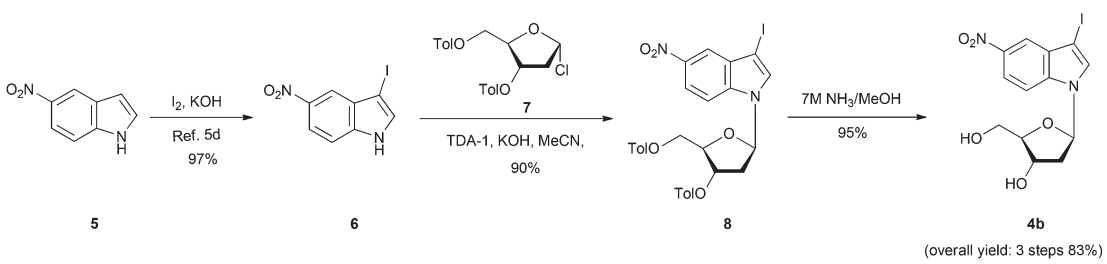

Scheme 1 Synthesis of 3-iodo-5-nitroindole nucleoside **4b**.

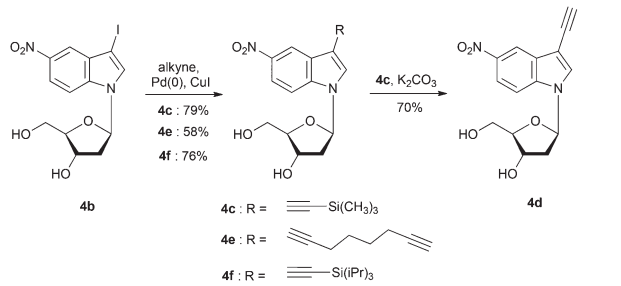

Scheme 2 Synthesis of 3-alkynyl modified 5-nitroindole nucleosides.

obtained in a straightforward manner in 58–79% yield. The silyl group of nucleoside **4c** was removed with K_2CO_3–MeOH in 70% yield (Scheme 2).

Next, phosphoramidite building blocks for solid-phase oligonucleotide synthesis were prepared. Nucleosides **4b**, **4d**, **4e** were converted to their 5′-*O*-(4,4′-dimethoxytrityl) derivatives **9b**, **9d**, **9e** in 54–61% yield, and phosphitylation under standard conditions furnished the phosphoramidites **10b**, **10d**, **10e** in 66–89% (Scheme 3).

The Sonogashira cross-coupling of the iodo nucleoside **4b** with trimethylsilylacetylene to the ethynyl nucleoside **4d** was reported earlier and was used to study the fidelity of triphosphate incorporation into oligonucleotides.[13] We synthesized compound **4d** with another palladium catalyst which resulted in a higher overall yield. Furthermore, in solid-phase oligonucleotide synthesis **4d** was not stable and converted into a by-product. We assigned the structure of the by-product, synthesized this compound and developed a protocol which circumvents side product formation (for details see the next section).

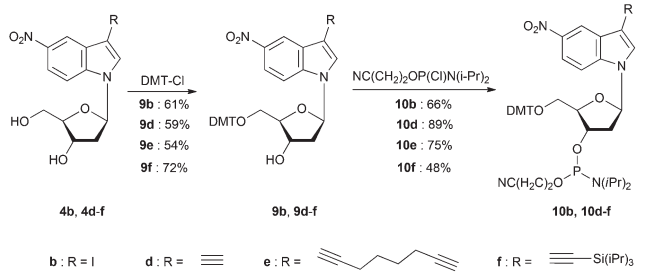

Scheme 3 Synthesis of phosphoramidite building blocks.

As we want to connect a highly fluorescent pyrene residue to the indole moiety, click functionalization was performed. To this end, 1-azidomethylpyrene **11** was prepared following an already published procedure.[16] The "click-reaction" was executed in the presence of $CuSO_4 \cdot 5H_2O$ with sodium ascorbate as reducing agent (Scheme 4). The corresponding dye conjugates **12** and **13** were obtained in 66% and 72% yield, respectively.

All new compounds were characterized by elemental analysis or mass spectra, as well as ^1H, ^{13}C and ^{31}P NMR spectra (Table S1†). The assignment of the ^1H- and ^{13}C-NMR chemical shifts for the 5-nitroindole derivatives were made by ^1H–^{13}C gated-decoupled spectra (Table S2†) as well as DEPT-135 (Distortionless Enhancement by Polarization Transfer) spectra and based on earlier findings.[17]

Synthesis of oligonucleotides and characterization of the side product formed by 4d

Oligonucleotides (ODNs) were prepared on solid-phase using the phosphoramidites **10d** and **10e** together with standard building blocks. Nucleosides **4d** and **4e** were incorporated in near central positions of the oligonucleotide 5′-d(TAGGTCA**A**-TACT) (ODN-**14**), thereby replacing particular dA residues. After solid-phase synthesis, the oligonucleotides were cleaved from the solid support and deprotected in concentrated aqueous ammonia at 55 °C for 16 h. Oligonucleotides were purified by reversed-phase HPLC (RP-18), detritylated with 2.5% dichloroacetic acid in dichloromethane and again purified by HPLC. The contents of single peaks were isolated in all cases (Fig. S1†). Subsequently, the molecular masses were determined by MALDI-TOF mass spectra (Table S3†).

Surprisingly, the mass of the isolated ODN-**15** (Table 1) was 18 units higher than calculated. Similar observations have been reported for a few other oligonucleotides containing 7-ethynyl-2′-deoxy-7-deazaguanosine, 5-ethynyl-2′-deoxycytidine and 5-ethynyl-2′-deoxyuridine.[18] However, hydration was not

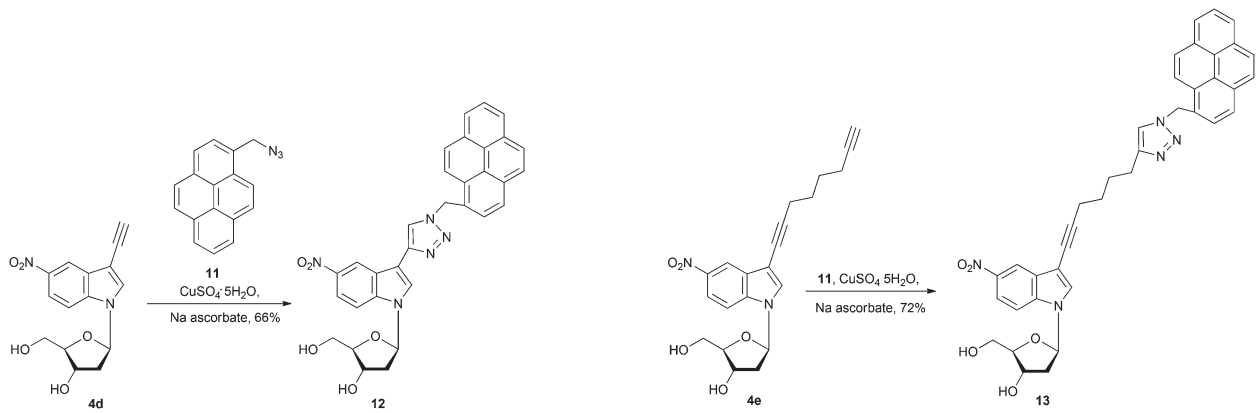

Scheme 4 Synthesis of nucleoside "click" conjugates.

Table 1 Thermal stabilities of modified 5-nitroindole oligonucleotides[a,b]

Duplexes	T_m [°C]	Duplexes	T_m [°C]	Duplexes	T_m [°C]	Duplexes	T_m [°C]	Duplexes	T_m [°C]
5′-d(TAG GTC **A**A**T** ACT) (**14**) 3′-d(ATC CAG T**T**A TGA) (**21**)	51	5′-d(TAG GTC A**4a**T ACT) (**26**) 3′-d(ATC CAG T**T**A TGA) (**21**)	42[c]	5′-d(TAG GTC A**4b**T ACT) (**27**) 3′-d(ATC CAG T**T**A TGA) (**21**)	43[d]	5′-d(TAG GTC A**4f**T ACT) (**28**) 3′-d(ATC CAG T**T**A TGA) (**21**)	38	5′-d(TAG GTC A**30**T ACT) (**29**) 3′-d(ATC CAG T**T**A TGA) (**21**)	33[e]
5′-d(TAG GTC **A**A**T** ACT) (**14**) 3′-d(ATC CAG T**C**A TGA) (**22**)	34	5′-d(TAG GTC A**4a**T ACT) (**26**) 3′-d(ATC CAG T**C**A TGA) (**22**)	45[c]	5′-d(TAG GTC A**4b**T ACT) (**27**) 3′-d(ATC CAG T**C**A TGA) (**22**)	43[d]	5′-d(TAG GTC A**4f**T ACT) (**28**) 3′-d(ATC CAG T**C**A TGA) (**22**)	38	5′-d(TAG GTC A**30**T ACT) (**29**) 3′-d(ATC CAG T**C**A TGA) (**22**)	34[e]
5′-d(TAG GTC **A**A**T** ACT) (**14**) 3′-d(ATC CAG T**A**A TGA) (**23**)	37	5′-d(TAG GTC A**4a**T ACT) (**26**) 3′-d(ATC CAG T**A**A TGA) (**23**)	44[c]	5′-d(TAG GTC A**4b**T ACT) (**27**) 3′-d(ATC CAG T**A**A TGA) (**23**)	43[d]	5′-d(TAG GTC A**4f**T ACT) (**28**) 3′-d(ATC CAG T**A**A TGA) (**23**)	37	5′-d(TAG GTC A**30**T ACT) (**29**) 3′-d(ATC CAG T**A**A TGA) (**23**)	34[e]
5′-d(TAG GTC **A**A**T** ACT) (**14**) 3′-d(ATC CAG T**G**A TGA) (**24**)	43	5′-d(TAG GTC A**4a**T ACT) (**26**) 3′-d(ATC CAG T**G**A TGA) (**24**)	41[c]	5′-d(TAG GTC A**4b**T ACT) (**27**) 3′-d(ATC CAG T**G**A TGA) (**24**)	42[d]	5′-d(TAG GTC A**4f**T ACT) (**28**) 3′-d(ATC CAG T**G**A TGA) (**24**)	36	5′-d(TAG GTC A**30**T ACT) (**29**) 3′-d(ATC CAG T**G**A TGA) (**24**)	33[e]
5′-d(TAG GTC **A**A**T** ACT) (**14**) 3′-r(AUC CAG UUA UGA) (**25**)	47	5′-d(TAG GTC A**4a**T ACT) (**26**) 3′-r(AUC CAG UUA UGA) (**25**)	n.m.	5′-d(TAG GTC A**4b**T ACT) (**27**) 3′-r(AUC CAG UUA UGA) (**25**)	n.m.	5′-d(TAG GTC A**4f**T ACT) (**28**) 3′-r(AUC CAG UUA UGA) (**25**)	30	5′-d(TAG GTC A**30**T ACT) (**29**) 3′-r(AUC CAG UUA UGA) (**25**)	n.m.
5′-d(TAG GTC A**4d**T ACT) (**17**) 3′-d(ATC CAG T**T**A TGA) (**21**)	41	5′-d(TAG GTC A**16**T ACT) (**15**) 3′-d(ATC CAG T**T**A TGA) (**21**)	41	5′-d(TAG GTC A**12**T ACT) (**18**) 3′-d(ATC CAG T**T**A TGA) (**21**)	41	5′-d(TAG GTC A**4e**T ACT) (**19**) 3′-d(ATC CAG T**T**A TGA) (**21**)	41	5′-d(TAG GTC A**13**T ACT) (**20**) 3′-d(ATC CAG T**T**A TGA) (**21**)	54
5′-d(TAG GTC A**4d**T ACT) (**17**) 3′-d(ATC CAG T**C**A TGA) (**22**)	42	5′-d(TAG GTC A**16**T ACT) (**15**) 3′-d(ATC CAG T**C**A TGA) (**22**)	41	5′-d(TAG GTC A**12**T ACT) (**18**) 3′-d(ATC CAG T**C**A TGA) (**22**)	40	5′-d(TAG GTC A**4e**T ACT) (**19**) 3′-d(ATC CAG T**C**A TGA) (**22**)	41	5′-d(TAG GTC A**13**T ACT) (**20**) 3′-d(ATC CAG T**C**A TGA) (**22**)	48
5′-d(TAG GTC A**4d**T ACT) (**17**) 3′-d(ATC CAG T**A**A TGA) (**23**)	42	5′-d(TAG GTC A**16**T ACT) (**15**) 3′-d(ATC CAG T**A**A TGA) (**23**)	41	5′-d(TAG GTC A**12**T ACT) (**18**) 3′-d(ATC CAG T**A**A TGA) (**23**)	40	5′-d(TAG GTC A**4e**T ACT) (**19**) 3′-d(ATC CAG T**A**A TGA) (**23**)	41	5′-d(TAG GTC A**13**T ACT) (**20**) 3′-d(ATC CAG T**A**A TGA) (**23**)	49
5′-d(TAG GTC A**4d**T ACT) (**17**) 3′-d(ATC CAG T**G**A TGA) (**24**)	39	5′-d(TAG GTC A**16**T ACT) (**15**) 3′-d(ATC CAG T**G**A TGA) (**24**)	39	5′-d(TAG GTC A**12**T ACT) (**18**) 3′-d(ATC CAG T**G**A TGA) (**24**)	40	5′-d(TAG GTC A**4e**T ACT) (**19**) 3′-d(ATC CAG T**G**A TGA) (**24**)	39	5′-d(TAG GTC A**13**T ACT) (**20**) 3′-d(ATC CAG T**G**A TGA) (**24**)	49
5′-d(TAG GTC A**4d**T ACT) (**17**) 3′-r(AUC CAG UUA UGA) (**25**)	34	5′-d(TAG GTC A**16**T ACT) (**15**) 3′-r(AUC CAG UUA UGA) (**25**)	35	5′-d(TAG GTC A**12**T ACT) (**18**) 3′-r(AUC CAG UUA UGA) (**25**)	30	5′-d(TAG GTC A**4e**T ACT) (**19**) 3′-r(AUC CAG UUA UGA) (**25**)	34	5′-d(TAG GTC A**13**T ACT) (**20**) 3′-r(AUC CAG UUA UGA) (**25**)	38

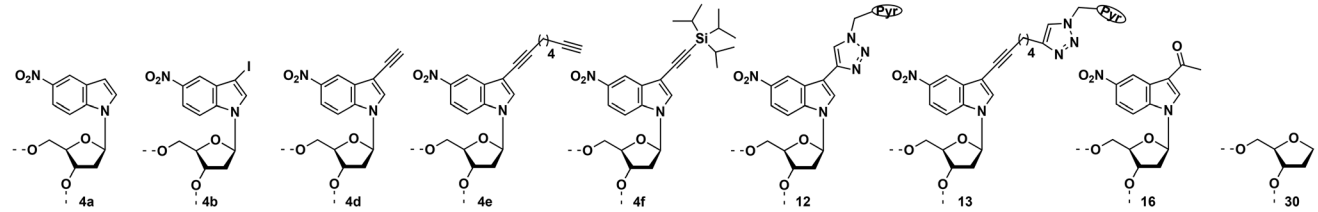

[a] Measured at 260 nm in 1 M NaCl, 100 mM $MgCl_2$, and 60 mM Na-cacodylate (pH 7.0) with 5 μM + 5 μM single-strand concentration. [b] T_m values were determined from the melting curves by using the software MELTWIN 3.0. n.m. = not measured. [c] Ref. 22. [d] Ref. 4*d*. [e] Ref. 3*c*.

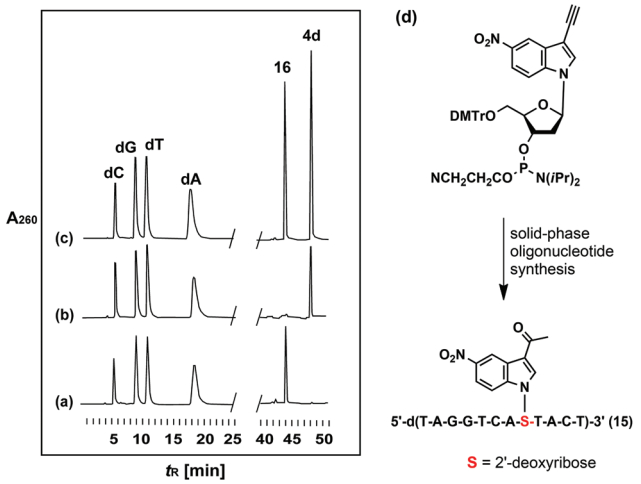

Fig. 2 HPLC profiles of the enzymatic hydrolysis products monitored at 260 nm: (a) 5′-d(TAG GTC A**16T** ACT) (ODN-**15**); (b) 5′-d(TAG GTC A**4dT** ACT) (ODN-**17**; after deprotection of TIPS group of ODN-**28**); (c) artificial mixture of 5′-d(TAG GTC A**16T** ACT) (ODN-**15**) + nucleosides **4d** and **16**; (d) hydration of ethynyl side chain during oligonucleotide synthesis.

observed for 7-ethynyl-2′-deoxy-7-deazaadenosine and 7-ethynyl-2′-deoxy-8-aza-7-deazaguanosine.[10e,18] Thus, we had to identify the side product from oligonucleotide synthesis. The presence of a side product was evidenced by enzymatic hydrolysis of ODN-**15** with snake-venom phosphodiesterase followed by alkaline phosphatase (for details, see Experimental section). The mixture obtained from the hydrolysis was analyzed by reversed-phase HPLC (RP-18, at 260 nm) showing the expected peaks for the canonical nucleosides and a side product (Fig. 2a and S2†). Moreover, the enzymatic digestion profile showed the absence of the ethynyl nucleoside **4d** indicating almost complete conversion to the side product (Fig. 2a).

As said before and according to the mass data, it was likely that the side product was formed by hydration. To verify the structure of the molecule, hydration of the monomeric 3-ethynyl-5-nitroindole **4d** was performed in MeOH–H_2O (9 : 1) containing a catalytic amount of H_2SO_4 (0.1 equivalents). By this, the acetyl nucleoside **16** was obtained exclusively (Scheme 5) and was identified on the basis of mass spectra, ^{1}H NMR and ^{13}C NMR chemical shifts (Table S1,† Experimental section). Treatment of **4d** with concentrated aqueous ammonia at 55 °C, as used during deprotection of oligonucleotides, did not lead to hydration (Fig. S3†).

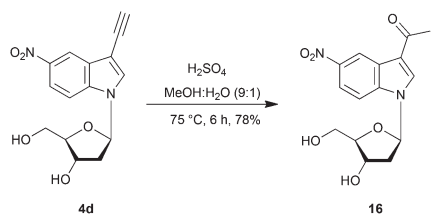

Scheme 5 Acid-catalyzed hydration reaction of ethynyl modified nucleoside **4d**.

To confirm ethynyl to acetyl conversion during oligonucleotide synthesis, the enzymatic hydrolysis mixture of ODN-**15** was co-injected together with the ethynylated nucleoside **4d** and the newly synthesized acetylated compound **16** (see Fig. 2c). The co-injected nucleoside matches the hydrolysis product (compare Fig. 2a and 2c). This result confirms that the by-product formed during oligonucleotide synthesis is the acetyl nucleoside **16** (Fig. 2d and Scheme 5).

To solve the problem of hydration, the ethynyl group was silylated with a hydrophobic triisopropylsilyl (TIPS) residue. The 3-TIPS-ethynylated nucleoside **4f** was synthesized from the 3-iodinated nucleoside **4b**, by the palladium catalyzed Sonogashira cross-coupling reaction with triisopropylsilylacetylene (Scheme 2). Then, compound **4f** was converted to the 5′-*O*-DMT derivative **9f** (72%) and was finally phosphitylated to afford **10f** in 48% yield (Scheme 3). The phosphoramidite **10f** was used together with unmodified building blocks in the synthesis of a TIPS ethynylated oligonucleotide (ODN-**28**) which was characterized by MALDI-TOF mass spectra (Table S3†). Then, the TIPS group of ODN-**28** was removed with tetrabutylammonium fluoride (TBAF) in CH_3CN–DMF (4 : 1) at room temperature for 16 h. The deprotected oligonucleotide was purified by reversed-phase HPLC. The exclusive formation of the ethynyl modified ODN-**17** was confirmed by MALDI-TOF mass spectra and enzymatic hydrolysis (Fig. 2b).

Next, a pyrene residue was introduced by post-modification.[19,20] For this, 'click' reactions were performed on ODN-**17** (short linker) or ODN-**19** (long linker) with 1-azidomethylpyrene (**11**) (Scheme 6) at room temperature in aqueous solution (for details see Experimental section). The pyrene residue makes the oligonucleotides rather lipophilic as indicated by their HPLC mobilities (Fig. S1†). The composition of oligonucleotides was confirmed by MALDI-TOF mass spectra (Table S3†).

Photophysical properties of nucleoside and oligonucleotide pyrene "click" conjugates with short and long linker arms

To evaluate the influence of the pyrene moiety connected *via* short and long linker arms to the indole skeleton, the UV/vis and fluorescence spectra of the nucleoside click conjugates **12** (short linker), **13** (long linker) as well as of oligonucleotide click adducts **18** and **20** were measured. The nucleoside pyrene "click" adducts **12** and **13**, show similar UV maxima (340 nm) and absorption pattern in the range of the pyrene absorbance (Fig. 3 and S4†). A 9 nm red shift is observed for pyrene in single stranded oligonucleotides (**18** and **20**) compared to nucleoside pyrene adducts **12** and **13** (Fig. 3). Upon duplex formation, a small bathochromic shift of the absorption maxima is observed (~1 to ~2 nm) compared to the single stranded oligonucleotide and a slightly reduced peak-to-valley ratio of the absorption bands. These phenomena point to pyrene intercalation among nucleobases of the oligonucleotide chain.

Next, the effect of the linker length on the fluorescence of the pyrene click adducts was studied (Fig. 4). The short (**12**)

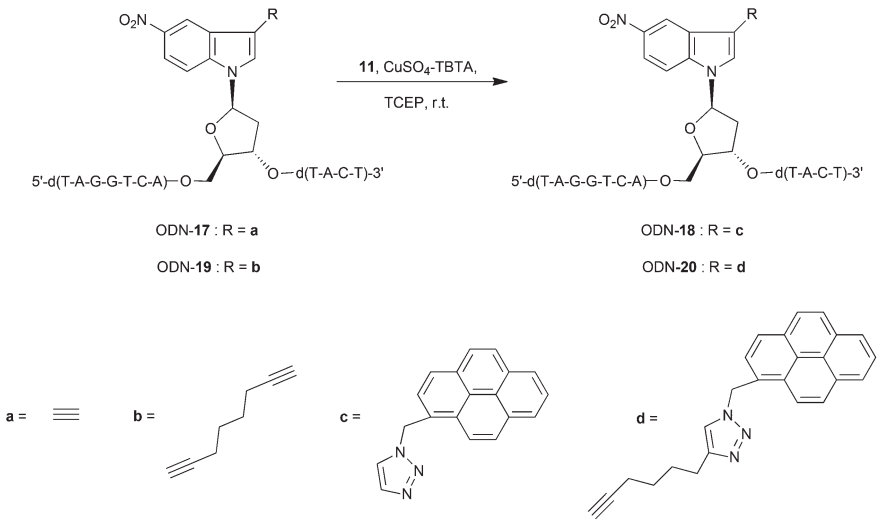

Scheme 6 Click reaction performed on oligonucleotides with 1-azidomethylpyrene.

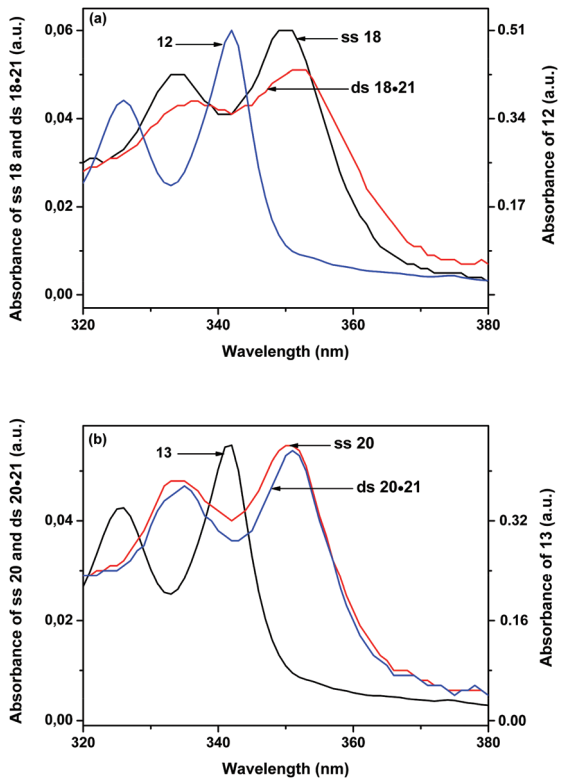

Fig. 3 Overlay of UV-vis spectra of (a) pyrene adduct **12**, ss-**18** and ds-**18**·**21**; (b) pyrene adduct **13**, ss-**20** and ds-**20**·**21**. The measurements were performed in 1 M NaCl, 100 mM $MgCl_2$, and 60 mM Na-cacodylate buffer (pH 7.0) for oligonucleotides (ss-**18**, ds-**18**·**21**, ss-**20** and ds-**20**·**21**, 2 μM) and methanol containing 1% DMSO for nucleosides (**12** and **13**, 10 μM). Right scale (absorbance) is for nucleosides and left scale is for oligonucleotides.

and long linker (**13**) conjugates bearing one pyrene residue show excitation maxima at 340 nm and monomeric pyrene emission maxima at 377 and 395 nm. The long linker pyrene click adduct **13** develops higher fluorescence intensity as the short linker pyrene click adduct **12** (Fig. 4). In both cases, the fluorescence of pyrene is strongly quenched by the 5-nitroindole moiety. This results from a photo-induced charge transfer from the dye and the indole moiety and depends on the redox potential.[21] For **12** and **13**, a hole transfer is considered forming a 5-nitroindole radical cation and a pyrene radical anion.[20,21g]

The fluorescence quenching of the long linker 5-nitroindole "click" adduct **13** was compared to other conjugates with various nucleobases (Fig. 4 and S5†). The comparison was made on nucleosides in order to exclude environmental changes occurring in the DNA. For this, the 7-deazaguanine pyrene conjugate **31**, 8-aza-7-deazaadenine pyrene conjugate **32** and abasic pyrene click conjugate **33** were selected.[20] According to Fig. 4, nucleobase controlled fluorescence quenching decreases in the following order: indole adduct **13** > 7-deazaguanine conjugate **31** > 8-aza-7-deazaadenine conjugate **32** > abasic linker conjugate **33**.

Afterwards, fluorescence properties of oligonucleotide pyrene conjugates were evaluated (Fig. 5). The fluorescence intensity of ss oligonucleotide **18** (short linker) was almost totally quenched by the 5-nitroindole moiety, while weak monomer emission fluorescence is observed for the ss oligonucleotide **20** containing long linker conjugate **13** (Fig. 5). This indicates that fluorescence quenching is linker dependent. This extraordinarily strong quenching might be different for other fluorescent dyes linked to the pyrrole moiety and showing a redox potential different from that of pyrene. In order to document universal base pairing character of the indole pyrene conjugate with regard to fluorescence changes, fluorescence spectra of the double stranded oligonucleotides were measured. To this end, oligonucleotide **20** (long linker) was hybridized with complementary strands positioning the four canonical bases opposite to the indole moiety (ds-**20**·**21**, ds-**20**·**22**, ds-**20**·**23**, ds-**20**·**24** and ds-**20**·**25**) (Fig. 5). A slight

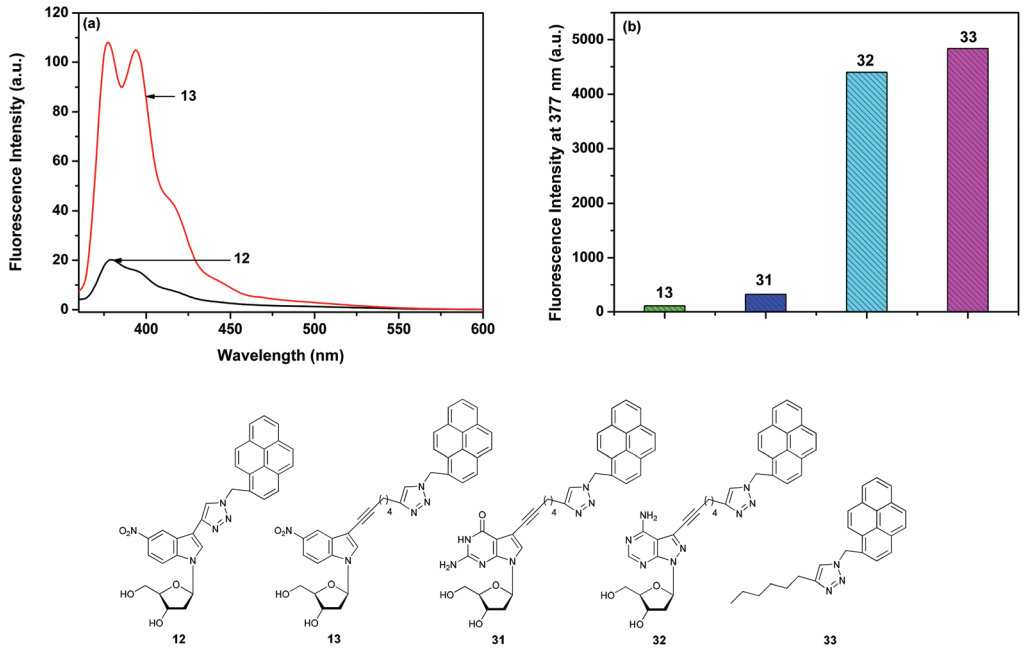

Fig. 4 (a) Fluorescence spectra of pyrene conjugates **12** and **13** (10 μM) in methanol. (b) Bar diagram showing the monomer emission fluorescence intensity (at 377 nm) of pyrene conjugates **13**, **31**–**33** (10 μM) in methanol. Excitation wavelength: 340 nm.

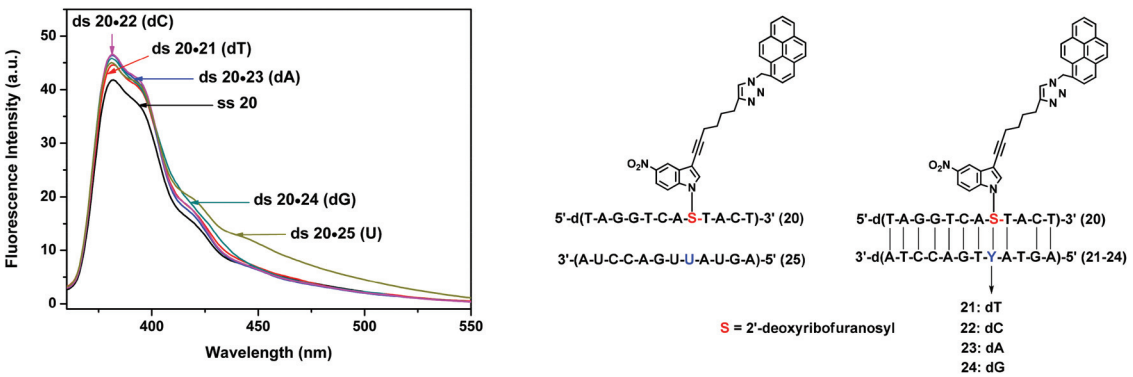

Fig. 5 Fluorescence emission spectra of 2 μM ss ODN-**20** and corresponding duplexes ds-**20**·**21**, ds-**20**·**22**, ds-**20**·**23**, ds-**20**·**24** and ds-**20**·**25** (2 μM of each strand), the measurements were performed in 1 M NaCl, 100 mM $MgCl_2$, and 60 mM Na-cacodylate buffer (pH 7.0). Excitation wavelength: 340 nm.

dequenching is observed from single strand to duplexes (Fig. 5). This effect was weaker than expected but might increase when dyes are used which do not interact as strongly as pyrene with DNA. The DNA-DNA duplexes as well as the DNA-RNA hybrids show almost identical fluorescence intensity. Thus, the change of canonical bases located opposite to the 5-nitroindole moiety has almost no influence on the fluorescence.

Universal base pairing properties of 3-substituted 5-nitroindole nucleosides in duplex DNA

The universal base pairing of 5-nitroindole oligonucleotides is well established. Several studies report that 5-nitroindole stabilizes duplex DNA by stacking interactions.[4] Destabilization was reported when the regioisomeric 4, 6 or 7-nitroindoles were incorporated in place of 5-nitroindole.[4a] Due to steric reasons, functionalization at the 3-position of indole are comparable to modifications at the 7-position of 7-deazapurines. In the previous section, the photophysical properties with regard to universal base pairing were studied. Now, universal base pairing properties of 3-substituted 5-nitroindole derivatives **4d–f**, **12**, **13** and **16** with regard to duplex stability are investigated and compared with those containing 5-nitroindole nucleosides **4a**, **4b**, and the abasic site **30** (Table 1).

In the first series of experiments (Table 1), the 3-substituted 5-nitroindole compounds **4d–f**, **16** or pyrene conjugates **12**, **13** were hybridized with oligonucleotides **21–25** containing the four canonical nucleosides in pairing positions. Then, melting curves were obtained under identical conditions and thermal

stabilities were compared to duplexes containing 5-nitroindole **4a**, **4b** or abasic site **30** at the same position.[3c,4d,22] From Table 1 it is apparent that all duplexes containing the 3-substituted 5-nitroindole nucleosides **4d**, **4e** and **16** show similar thermal stabilities when located opposite to all four canonical bases compared to the parent oligonucleotides incorporating **4a** or **4b**. This indicates that universal base pairing is maintained for all 3-substituted 5-nitroindole nucleosides (Table 1). Only the hydrophobic triisopropylsilyl protecting group causes duplex destabilization (**4f**) but still shows universal base pairing. Compared to these results, the abasic **30** (1,2-dideoxyribosefuranose without nucleobase) led to strongly decreased T_m values.[3c] Hybridization experiments were also performed with the complementary RNA strand ODN-**25** and it was observed that thermal stability of the DNA-RNA hybrids is significantly lower than for DNA-DNA duplexes (Table 1).

Next, the influence of the pyrene residue on duplex stability was studied with ODN-**20** containing the long linker pyrene conjugate **13**. The pyrene residue of ODN-**20** stabilizes universal base pairs significantly. An additional stabilization opposite to dT was observed (Table 1). On the contrary an increase in duplex stability is not observed for the short linker pyrene click adduct **12** neither with DNA nor with RNA. The intercalation ability of pyrene has been accounted for duplex stabilization.[23] Thus, molecular dynamics simulation studies using Amber force field were performed (Hyperchem 8.0) (Fig. 6) to visualize the interactions of the 5-nitroindole dye conjugates **12** (short linker) and **13** (long linker) in DNA duplexes. The studies were made on the 12-mer duplexes **18**·**21** and **20**·**21** (Fig. 6a and b). The energy minimized molecular structures were built as B-type DNA, and the duplex structure was kept intact after introduction of the modifications. Fig. 6a displays duplex **18**·**21** bearing the short linker adduct **12**, while Fig. 6b shows duplex **20**·**21** containing long linker adduct **13**.

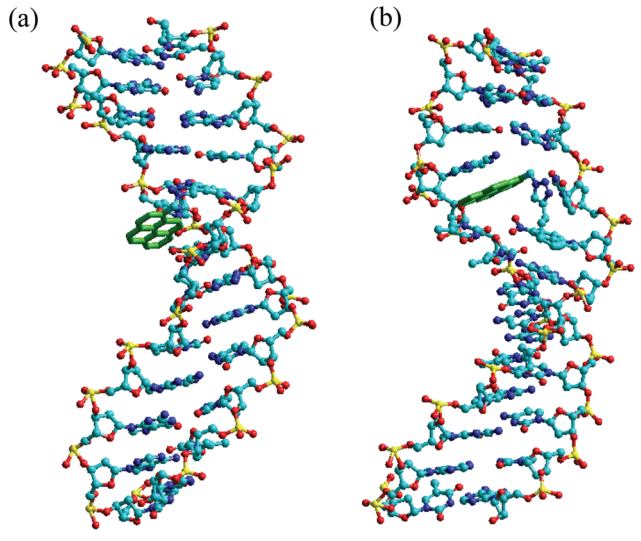

Fig. 6 Molecular models of (a) duplex 5′-d(TAG GTC A**12T** ACT) (**18**)·3′-d(ATC CAG TTA TGA) (**21**) and (b) duplex 5′-d(TAG GTC A**13T** ACT) (**20**)·3′-d(ATC CAG TTA TGA) (**21**). The models were constructed using Hyperchem 8.0 and energy minimized using AMBER calculations.

According to the modelling studies, the pyrene residue of long linker adduct **13** intercalates in the B-DNA structure (Fig. 6b), while the pyrene residue of the short linker adduct **12** is located in the major groove not showing intercalation (Fig. 6a). Hence, the location of the pyrene residue in the DNA structure strongly depends on the linker length. The universal base pairing properties as well as the higher thermal stability of the long linker 5-nitroindole pyrene adduct have the potential to increase primer probe interactions used in diagnostic applications.

Conclusion

5-Nitroindole oligonucleotides with clickable short (**4d**) and long linkers (**4e**) were synthesized by solid-phase synthesis. To this end, corresponding phosphoramidites (**10d–e**) were prepared. For large scale glycosylation of the iodo base **6**, KOH and phase-transfer conditions were used. The 3-ethynyl-5-nitroindole residue **4d** was hydrated during solid-phase oligonucleotide synthesis to the 3-acetyl-5-nitroindole nucleoside **16** which was unambiguously characterized. By-product formation was circumvented by temporary triisopropylsilyl protection of the ethynyl side chain.

Oligonucleotide duplexes with 3-ethynyl, 3-acetyl and 3-octadiynyl-5-nitroindoles (**4d**, **16**, **4e**) incorporated opposite to the four canonical DNA nucleosides showed the same universal base pairing behavior as those with the non-functionalized **4a**. Copper(I)-catalyzed cycloaddition of octadiynylated and ethynylated oligonucleotides with 1-azidomethylpyrene **11** yielded oligonucleotides containing pyrene residues attached to 5-nitroindole by short and long linker arms. In all cases, fluorescence was strongly quenched. A single replacement of a canonical nucleoside by a long linker pyrene adduct **13** stabilizes the duplex substantially, most likely by intercalation of the pyrene residue as verified by molecular modelling studies. The universal base pairing properties as well as the higher thermal stability of the long linker 5-nitroindole pyrene adduct have the potential to increase primer probe interactions in diagnostic assays. The combination of universal base pairing and strong dye quenching in the same molecule might be used to detect hybridization by fluorescence increase or to study charge transfer in DNA. All compounds with a clickable 5-nitroindole skeleton show universal base pairing and can be functionalized with almost any azide in any position of the DNA chain.

Experimental section

3-Iodo-5-nitroindole (6)

Prepared according to ref. 5*d*. λ_{max} (MeOH)/nm: 270 (ε/dm^3 mol^{-1} cm^{-1} 16 900), 319 (16 900). ^{1}H NMR (DMSO-d_6, 300 MHz) δ 7.58 (d, J = 2.2 Hz, 1H, H-7), 7.84 (s, 1H, H-2), 8.02

(d, J = 2.1 Hz, 1H, H-6), 8.16 (s, 1H, H-4), 12.22 (s, 1H, NH). ^{13}C NMR (DMSO-d_6, 75 MHz) δ 58.8, 112.7, 116.8, 117.5, 129.1, 133.9, 139.4, 141.4. For ^{1}H-NMR data see also ref. 12*a* and 13. Anal. Calcd for $C_8H_5IN_2O_2$ (288.04): C, 33.36; H, 1.75; N, 9.73. Found: C, 33.25; H, 1.76; N, 9.68.

1-(2-Deoxy-3,5-(di-*O*-4-methylbenzoyl)-β-D-*erythro*-pentofuranosyl)-3-iodo-5-nitroindole (8). Powdered KOH (23.5 g, 0.42 mol) and TDA-1 (tris[2-(2-methoxyethoxy)ethyl]amine (5 mL, 15 mmol) were suspended in dry MeCN (500 mL), and the suspension was stirred for 5 min at room temperature. Then, **6** (42 g, 0.15 mol) was added and stirring was continued for 10 min. Compound **7**[14b] (61.6 g, 0.16 mol) was added in portions, and the reaction mixture was stirred for 20 min at room temperature by cooling. Insoluble material was filtered off and the filtrate was evaporated until crystallization started. The crystalline material was filtered off and washed with MeCN. The filtrate was evaporated to near dryness, then ethanol was added and the crystalline precipitate was filtered off. This procedure was repeated several times until the reaction product was not detectable anymore in the TLC of the filtrate. The combined crystalline materials were collected and dried furnishing **8** (86.5 g, 90%). TLC (PE–EtOAc, 80 : 20) R_f 0.5. λ_{max} (MeOH)/nm 242 (ε/dm^3 mol^{-1} cm^{-1} 38 400), 272 (22 500), 318 (7000). ^{1}H NMR (DMSO-d_6, 300 MHz) δ 2.36, 2.39 (2s, 6H, 2× CH_3), 2.73–2.81 (m, 1H, H_α-2′), 2.93–3.03 (m, 1H, H_β-2′), 4.49–4.64 (m, 3H, 2× H-5′, H-4′), 5.70–5.72 (m, 1H, H-3′), 6.70 (t, J = 6.3 Hz, 1H, H-1′), 7.29–7.37 (m, 4H, Ar–H), 7.82–8.12 (m, 8H, Ar–H). ^{13}C NMR (DMSO-d_6, 75 MHz) δ 21.2, 21.3, 36.6, 61.3, 64.0, 74.7, 81.5, 85.3, 111.9, 117.1, 117.9, 126.4, 126.5, 129.2, 129.3, 129.4, 129.6, 130.1, 132.9, 139.0, 142.0, 143.9, 144.1, 165.3, 165.5. Anal. Calcd for $C_{29}H_{25}I\,N_2O_7$ (640.42): C, 54.39; H, 3.93; N, 4.37. Found: C, 54.28; H, 3.95; N, 4.40.

1-(2-Deoxy-β-D-*erythro*-pentofuranosyl)-3-iodo-5-nitroindole (4b). Compound **8** (53.4 g, 0.083 mol) was treated with 7 M NH_3–MeOH (2 L), and the suspension was stirred at ambient temperature until a clear solution was obtained (~24 h). The solution was evaporated to dryness and the remaining residue was treated with CH_2Cl_2 (250 mL). The resulting precipitate was filtrated and washed with CH_2Cl_2 (2 × 50 mL). Compound **4b** was obtained as yellow crystalline compound (32 g, 95%). TLC (CH_2Cl_2–MeOH, 90 : 10) R_f 0.5. λ_{max} (MeOH)/nm 273 (ε/dm^3 mol^{-1} cm^{-1} 16 800), 319 (5600). ^{1}H NMR (DMSO-d_6, 300 MHz) δ 2.26–2.33 (m, 1H, H_α-2′), 2.44–2.53 (m, 1H, H_β-2′), 3.54–3.55 (m, 2H, 2× H-5′), 3.84–3.87 (m, 1H, H-4′), 4.36–4.38 (m, 1H, H-3′), 5.00 (br s, 1H, HO-5′), 5.37 (br s, 1H, HO-3′), 6.45 (t, J = 6.6 Hz, 1H, H-1′), 7.83 (d, J = 9.1 Hz, 1H, H-7), 8.03–8.11 (m, 3H, Ar–H). ^{13}C NMR (DMSO-d_6, 75 MHz) δ 60.4, 61.5, 70.5, 85.2, 87.6, 111.7, 117.0, 117.8, 129.9, 133.4, 138.9, 141.8. For ^{1}H-NMR data see also ref. 13. Anal. Calcd for $C_{13}H_{13}I\,N_2O_5$ (404.16): C, 38.63; H, 3.24; N, 6.93. Found: C, 38.73; H, 3.25; N, 6.90.

1-[2-Deoxy-5-*O*-(4,4′-dimethoxytrityl)-β-D-*erythro*-pentofuranosyl]-3-iodo-5-nitroindole (9b). Compound **4b** (3.0 g, 7.4 mmol) was co-evaporated with pyridine (3 × 10 mL) and then dissolved in pyridine (20 mL). Then, 4,4′-dimethoxytritylchloride (3.0 g, 8.7 mmol) was added. The reaction mixture was stirred for 3 h at room temperature, CH_2Cl_2 (25 mL) was added and the solution was poured into 5% $NaHCO_3$ solution (30 mL). The aqueous layer was extracted with dichloromethane (30 mL), the combined organic layers were washed with brine, dried (Na_2SO_4), filtered and the solvent was evaporated. The resulting oil was co-evaporated with toluene (3 × 20 mL each) and acetone (1 × 20 mL) furnishing a yellow foam which was applied to FC (silica gel, column 10 × 5 cm, CH_2Cl_2→CH_2Cl_2–acetone 95 : 5). Evaporation of the main fraction afforded **9b** as white foam (3.2 g, 61%). TLC (CH_2Cl_2–acetone, 90 : 10) R_f 0.7. λ_{max} (MeOH)/nm 233 (ε/dm^3 mol^{-1} cm^{-1} 25 500), 274 (21 000), 319 (5900). ^{1}H NMR (DMSO-d_6, 300 MHz) δ 2.35–2.43 (m, 1H, H_α-2′), 2.63–2.72 (m, 1H, H_β-2′), 3.13–3.14 (m, 2H, H-5′), 3.71 (s, 6H, 2 × OCH_3), 3.96–4.00 (m, 1H, H-4′), 4.44–4.48 (m, 1H, H-3′), 5.41 (d, J = 6.1 Hz, 1H, HO-3′), 6.51 (t, J = 6.1 Hz, 1H, H-1′), 6.77–6.11 (m, 4H, Ar–H), 7.17–7.33 (m, 9H, Ar–H), 7.91 (d, J = 9.3 Hz, 1H, H-7), 8.02–8.07 (m, 2H, H-2, H-6), 8.17 (d, J = 2.0 Hz, 1H, H-4). ^{13}C NMR (DMSO-d_6, 75 MHz) δ 55.0, 60.3, 60.4, 63.6, 70.2, 85.2, 85.5, 85.6, 112.2, 113.1, 117.1, 117.8, 126.6, 127.7, 127.8, 129.6, 129.7, 130.2, 133.2, 135.4, 135.5, 138.9, 141.9, 144.7, 158.9, 158.0. Anal. Calcd for $C_{34}H_{31}IN_2O_7$ (706.52): C, 57.80; H, 4.42; N, 3.96. Found: C, 58.01; H, 4.60; N, 4.05.

1-[2-Deoxy-5-*O*-(4,4′-dimethoxytrityl)-β-D-*erythro*-pentofuranosyl]-3-iodo-5-nitroindole 3′-[(2-cyanoethyl)-(*N*,*N*-diisopropyl)]-phosphoramidite (10b). Compound **9b** (1.5 g, 2.12 mmol) was dissolved in dry CH_2Cl_2 (20 mL). The mixture was treated with *N*,*N*-diisopropylethylamine (690 μL, 3.86 mmol) and 2-cyanoethyldiisopropylphosphoramido chloridite (690 μL, 3.08 mmol). The resulting mixture was stirred for 20 min at room temperature, then the solution was diluted with CH_2Cl_2 (10 mL) and poured into 50 ml 5% $NaHCO_3$ solution. The aqueous layer was extracted with CH_2Cl_2 (3 × 50 mL), the combined organic layers were dried (Na_2SO_4), filtrated and evaporated. The residual foam was purified by FC (silica gel, column 8 × 4 cm, CH_2Cl_2→CH_2Cl_2–acetone 99 : 1). Evaporation of the main fraction afforded **10b** (1.26 g, 66%) as yellow foam. TLC (CH_2Cl_2–acetone, 98 : 2) R_f 0.7. ^{31}P-NMR (121.5 MHz, $CDCl_3$) δ 148.8, 148.7. Anal. calcd for $C_{43}H_{48}IN_4O_8P$ (906.74): C, 56.96; H, 5.34; N, 6.18. Found: C, 56.68; H, 5.31; N, 6.21.

1-(2-Deoxy-β-D-*erythro*-pentofuranosyl)-3-[(trimethylsilyl)-acetylene]-5-nitroindole (4c). Compound **4b** (1.5 g, 3.7 mmol) was dissolved in anhydrous DMF (10 mL), then CuI (0.380 g, 0.2 mmol), tetrakis(triphenylphosphine) Pd(0) (1.16 g, 0.1 mmol), triethylamine (1.0 mL, 0.7 g, 7.5 mmol) and trimethylsilylacetylene (5.0 mL, 3.5 g, 36 mmol) were introduced. The solution was stirred at rt overnight. The solvent was removed under vacuo, and the resulting oily residue was co-evaporated with toluene twice (2 × 20 mL), adsorbed on silica gel and applied to FC (silica gel, column 25 × 5 cm, CH_2Cl_2→CH_2Cl_2–MeOH, 90 : 10). Evaporation of the main fraction afforded **4c** (1.1 g, 79%) as yellow solid. TLC (CH_2Cl_2–MeOH, 90 : 10) R_f 0.5. λ_{max} (MeOH)/nm 248 (ε/dm^3 mol^{-1} cm^{-1} 20 800), 254 (21 400), 276 (22 600), 320 (8800). ^{1}H NMR (DMSO-d_6, 300 MHz) δ 0.28 (s, 9H, CH_3), 2.27–2.35 (m, 1H, H_α-

2′), 2.45–2.54 (m, 1H, H_β-2′), 3.50–3.58 (m, 2H, 2× H-5′), 3.85–3.89 (m, 1H, H-4′), 4.36–4.39 (m, 1H, H-3′), 5.00 (t, J = 5.4 Hz, 1H, HO-5′), 5.35 (d, J = 4.2 Hz, 1H, HO-3′), 6.46 (t, J = 6.6 Hz, 1H, H-1′), 7.91 (d, J = 9.0 Hz, 1H, H-7), 8.10 (dd, J = 2.4 Hz, 9.3 Hz, 1H, H-2), 8.27 (s, 1H, H-6), 8.35 (d, J = 2.4 Hz, 1H, H-4). ^{13}C NMR (DMSO-d_6, 75 MHz) δ 61.4, 70.5, 85.3, 87.7, 97.1, 97.5, 99.5, 112.0, 115.4, 118.1, 128.1, 133.5, 137.7, 141.9. For ^{1}H-NMR data see also ref. 13. Anal. Calcd for $C_{18}H_{22}N_2O_5Si$ (374.46): C, 57.73; H, 5.92; N, 7.48. Found: C, 57.85; H, 5.85; N, 7.44.

1-(2-Deoxy-β-D-*erythro*-pentofuranosyl)-3-ethynyl-5-nitroindole (4d). Compound **4c** (0.810 g, 2.2 mmol) was dissolved in MeOH (20 mL). Then, potassium carbonate (0.1 g, 0.72 mmol) was added and the suspension was stirred for 12 h, filtered and the filtrate was evaporated under vacuo. The remaining residue was adsorbed on silica gel and applied to FC (silica gel, column 20 × 5 cm, CH_2Cl_2→CH_2Cl_2–MeOH, 90 : 10). Evaporation of the main fraction afforded **4d** (0.460 g, 70%) as yellow solid. TLC (CH_2Cl_2–MeOH, 95 : 5) R_f 0.5. λ_{max} (MeOH)/nm 260 (ε/dm^3 mol^{-1} cm^{-1} 16 000), 273 (22 000), 319 (7300). ^{1}H NMR (DMSO-d_6, 300 MHz) δ 2.28–2.36 (m, 1H, H_α-2′), 2.45–2.54 (m, 1H, H_β-2′), 3.51–3.61 (m, 2H, 2× H-5′), 3.85–3.89 (m, 1H, H-4′), 4.35–4.40 (m, 2H, C≡CH, H-3′), 5.01 (t, J = 5.1 Hz, 1H, HO-5′), 5.36 (d, J = 4.2 Hz, 1H, HO-3′), 6.46 (t, J = 6.6 Hz, 1H, H-1′), 7.91 (dd, J = 9.0 Hz, 1.5 Hz, 1H, H-7), 8.09 (dd, J = 9.3 Hz, 1.5 Hz, 1H, H-2), 8.26 (s, 1H, H-6), 8.38 (d, J = 1.5 Hz, 1H, H-4). ^{13}C NMR (DMSO-d_6, 75 MHz) δ 61.4, 70.5, 75.6, 83.9, 85.3, 87.7, 98.9, 112.0, 115.5, 118.0, 128.3, 133.4, 137.7, 142.0. For ^{1}H-NMR data see also ref. 13. Anal. Calcd for $C_{15}H_{14}N_2O_5$ (302.09): C, 59.60; H, 4.67; N, 9.27. Found: C, 59.89; H, 4.73; N, 9.21.

1-[2-Deoxy-5-*O*-(4,4′-dimethoxytrityl)-β-D-*erythro*-pentofuranosyl]-3-ethynyl-5-nitroindole (9d). Compound **4d** (0.360 g, 1.2 mmol) was co-evaporated with pyridine (3 × 10 mL) and dissolved in pyridine (20 mL). Then 4,4′-dimethoxytritylchloride (1.5 g, 4.4 mmol) was added. The reaction mixture was stirred overnight at rt, then CH_2Cl_2 (25 mL) was added and the solution was poured into 5% $NaHCO_3$ solution (30 mL). The aqueous layer was extracted two times with dichloromethane (30 mL), the combined organic layers were washed with a saturated NaCl solution, dried (Na_2SO_4), filtered and the solvent was evaporated. The resulting oil was co-evaporated with toluene (3 × 20 mL) and acetone (1 × 20 mL) giving a yellow foam which was applied to FC (silica gel, column 15 × 5 cm, CH_2Cl_2→CH_2Cl_2–acetone, 98 : 2). Evaporation of the main fraction afforded **9d** as yellow foam (0.430 g, 59%). TLC (CH_2Cl_2–acetone, 95 : 5) R_f 0.7. λ_{max} (MeOH)/nm 235 (ε/dm^3 mol^{-1} cm^{-1} 34 700), 275 (26 900), 321 (6800). ^{1}H NMR (DMSO-d_6, 300 MHz) δ 2.37–2.42 (m, 1H, H_α-2′), 2.67–2.72 (m, 1H, H_β-2′), 3.10–3.12 (m, 2H, 2× H-5′), 3.70 (s, 6H, 2× OCH_3), 3.96–3.97 (m, 1H, H-4′), 4.38 (s, 1H, C≡CH), 4.44–4.47 (m, 1H, H-3′), 5.41 (d, J = 4.8 Hz, 1H, HO-3′), 6.51 (t, J = 6.0 Hz, 1H, H-1′), 6.75–6.79 (m, 4H, Ar–H), 7.13–7.29 (m, 9H, Ar–H), 7.95 (d, J = 9.3 Hz, 1H, H-7), 8.07 (dd, J = 2.1 Hz, 9.3 Hz, 1H, H-6), 8.19 (s, 1H, H-2), 8.41 (d, J = 2.1 Hz, 1H H-4). ^{13}C NMR (DMSO-d_6, 75 MHz) δ 54.9, 55.0, 63.5, 69.9, 75.6, 83.9, 85.1, 85.4, 85.6, 98.8, 112.5, 113.1, 115.5, 118.0, 126.6, 127.6, 127.7, 128.5, 129.6, 129.7, 133.2, 135.4, 135.5, 137.9, 142.0, 144.7, 157.9, 158.0. Anal. Calcd for $C_{36}H_{32}N_2O_7$ (604.65): C, 71.51; H, 5.33; N, 4.63. Found: C, 71.60; H, 5.33; N, 4.63.

1-[2-Deoxy-5-*O*-(4,4′-dimethoxytriphenylmethyl)-β-D-*erythro*-pentofuranosyl]-3-ethynyl-5-nitroindole 3′-[(2-Cyanoethyl)-(*N*,*N*-diisopropyl)]-phosphoramidite (10d). Compound **9d** (0.350 g, 0.58 mmol) was dissolved in anh. CH_2Cl_2 (10 mL). The mixture was treated with *N*,*N*-diisopropylethylamine (193 µL, 1.1 mmol) and 2-cyanoethyldiisopropylphosphoramidochloridite (193 µL, 0.56 mmol) for 20 min at rt. The solution was diluted with CH_2Cl_2 (20 mL) and poured into a 5% $NaHCO_3$ solution (50 mL). The aq. layer was extracted with CH_2Cl_2 (3 × 50 mL), the combined organic layers were dried (Na_2SO_4), filtrated and evaporated. The residual foam was purified by FC (silica gel, column 8 × 4 cm, PE–EtOAc, 1 : 1). Evaporation of the main fraction afforded 10d (0.417 g, 89%) as yellow foam. TLC (PE–EtOAc, 1 : 1) R_f 0.7. ^{31}P NMR ($CDCl_3$, 121.5 MHz) δ 148.92, 148.87. Anal. Calcd for $C_{45}H_{49}N_4O_8P$ (804.87): C, 67.15; H, 6.14; N, 6.96. Found: C, 67.12; H, 6.00; N, 6.87.

1-(2-Deoxy-β-D-*erythro*-pentofuranosyl)-3-(octa-1,7-diynyl)-5-nitroindole (4e). Compound **4b** (2 g, 4.9 mmol) was dissolved in anhydrous DMF (10 mL), then CuI (0.500 g, 0.05 mmol) tetrakis(triphenylphosphine) Pd(0) (1.2 g, 0.1 mmol), triethylamine (1.3 mL, 0.9 g, 9.8 mmol) and octa-1,7-diyne (6.0 mL, 4.9 g, 46 mmol) were introduced. The solution was stirred for 1 h at rt. The solvent was removed under vacuo, and the resulting oily residue was co-evaporated with toluene twice (2 × 20 mL), adsorbed on silica gel and applied to FC (silica gel, column 25 × 5 cm, CH_2Cl_2→CH_2Cl_2–MeOH, 90 : 10). Evaporation of the main fraction afforded **4e** (1.1 g, 58%) as yellow solid. TLC (CH_2Cl_2–MeOH, 9 : 1) R_f 0.6. λ_{max} (MeOH)/nm 260 (ε/dm^3 mol^{-1} cm^{-1} 12 700), 278 (21 100), 320 (7500). ^{1}H NMR (DMSO-d_6, 300 MHz) δ 1.63–1.67 (m, 4H, 2 × CH_2), 2.23–2.34 (m, 3H, H_α-2′, CH_2), 2.45–2.57 (m, 3H, H_β-2′, CH_2), 2.78–2.79 (m, 1H, C≡CH), 3.49–3.62 (m, 2H, 2× H-5′), 3.84–3.87 (m, 1H, H-4′), 4.36–4.39 (m, 1H, H-3′), 5.00 (t, J = 5.0 Hz, 1H, HO-5′), 5.35 (d, J = 3.6 Hz, 1H, HO-3′), 6.46 (t, J = 6.5 Hz, 1H, H-1′), 7.88 (d, J = 9.2 Hz, 1H, H-7), 8.07–8.11 (m, 1H, H-2), 8.13 (s, 1H, H-6), 8.38 (d, J = 1.6 Hz, 1H, H-4). ^{13}C NMR (DMSO-d_6, 75 MHz) δ 17.3, 18.4, 27.2, 27.4, 61.5, 70.5, 71.3, 72.0, 84.3, 85.1, 87.6, 93.2, 100.4, 111.7, 115.5, 117.8, 128.3, 131.8, 137.8, 141.7. ESI-TOF m/z calcd for $C_{21}H_{22}N_2O_5$ $[M + Na]^+$ 405.1421, found 405.1427.

1-[2-Deoxy-5-*O*-(4,4′-dimethoxytrityl)-β-D-*erythro*-pentofuranosyl)-3-(octa-1,7-diynyl)-5-nitroindole (9e). Compound **4e** (0.700 g, 1.8 mmol) was co-evaporated with pyridine (3 × 10 mL) and dissolved in pyridine (20 mL). Then 4,4′-dimethoxytritylchloride (0.805 g, 2.4 mmol) was added. The reaction mixture was stirred for 4 h at rt, then CH_2Cl_2 (25 mL) was added and the solution was poured into a 5% $NaHCO_3$ solution (30 mL). The aqueous layer was extracted two times with dichloromethane (2 × 30 mL), the combined organic layers were washed with a saturated NaCl solution, dried (Na_2SO_4), filtered and the solvent was evaporated. The resulting oil was

co-evaporated with toluene (3 × 20 mL) giving a yellow foam which was applied to FC (silica gel, column 10 × 5 cm, PE–EtOAc, 1 : 1). Evaporation of the main fraction afforded **9e** as yellow foam (0.670 g, 54%). TLC (PE–EtOAc, 1 : 1) R_f 0.5. λ_{max} (MeOH)/nm 234 (ε/dm^3 mol^{-1} cm^{-1} 33 800), 278 (22 300), 321 (9700). ^{1}H NMR (DMSO-d_6, 300 MHz) δ 1.57–1.69 (m, 4H, 2 × CH_2), 2.20–2.26 (m, 2H, CH_2), 2.33–2.41 (m, 1H, H_α-2′), 2.48–2.55 (m, 4H, 2 × CH_2), 2.63–2.71 (m, 1H, H_β-2′), 2.78 (t, J = 2.7 Hz, 1H, C≡CH), 3.11–3.12 (m, 2H, 2× H-5′), 3.70 (s, 6H, 2 × OCH_3), 3.94–3.98 (m, 1H, H-4′), 4.40–4.46 (m, 1H, H-3′), 5.39 (d, J = 4.8 Hz, 1H, HO-3′), 6.49 (t, J = 6.0 Hz, 1H, H-1′), 6.76–6.78 (m, 4H, Ar–H), 7.14–7.31 (m, 9H, Ar–H), 7.92 (d, J = 9.3 Hz, 1H, H-7), 8.03–8.07 (m, 2H, H-2, H-6), 8.39 (d, J = 2.1 Hz, 1H, H-4). ^{13}C NMR (DMSO-d_6, 75 MHz) δ 17.3, 18.4, 27.2, 27.4, 54.9, 63.6, 70.0, 71.3, 72.0, 84.3, 85.0, 85.4, 85.6, 93.2, 100.4, 112.2, 113.1, 115.5, 117.8, 126.6, 127.6, 127.8, 128.5, 129.7, 131.8, 135.3, 135.4, 137.9, 141.8, 144.8, 158.0. ESI-TOF m/z calcd for $C_{42}H_{40}N_2O_7$ [M + Na]$^+$ 707.2728, found 707.2721.

1-[2-Deoxy-5-*O*-(4,4′-dimethoxytrityl)-β-D-*erythro*-pentofuranosyl)-3-(octa-1,7-diynyl)-5-nitroindole 3′-[(2-Cyanoethyl)-(*N*,*N*-diisopropyl)]-phosphoramidite (10e). Compound **9e** (0.500 g, 0.73 mmol) was dissolved in anh. CH_2Cl_2 (10 mL). The mixture was treated with *N*,*N*-diisopropylethylamine (243 μL, 1.4 mmol) and 2-cyanoethyl diisopropylphosphoramidochloridite (243 μL, 0.71 mmol) for 20 min at rt. The solution was diluted with CH_2Cl_2 (20 mL) and poured into a 5% $NaHCO_3$ solution (50 mL). The aq. layer was extracted with CH_2Cl_2 (3 × 50 mL), the combined organic layers were dried (Na_2SO_4), filtrated and evaporated. The residual foam was purified by FC (silica gel, column 8 × 4 cm, PE–EtOAc, 1 : 1). Evaporation of the main fraction afforded **10e** (0.483 g, 75%) as yellow foam. TLC (PE–EtOAc, 20 : 10) R_f 0.6. ^{31}P NMR ($CDCl_3$, 121.5 MHz) δ 148.92, 148.89. Anal. Calcd for $C_{51}H_{57}N_4O_8P$ (884.99): C, 69.29; H, 6.49; N, 6.33. Found C, 69.29; H, 6.37; N, 6.12.

1-(2-Deoxy-β-D-*erythro*-pentofuranosyl)-3-[(triisopropylsilyl)-ethynyl]-5-nitroindole (4f). Compound **4b** (0.200 g, 0.5 mmol) was dissolved in anhydrous DMF (3 mL), then CuI (0.019 g, 0.1 mmol), tetrakis(triphenylphosphine) Pd(0) (0.058 g, 0.05 mmol), triethylamine (130 μL, 1 mmol) and triisopropylsilylacetylene (280 μL, 0.228 g, 1.25 mmol) were introduced. The solution was stirred under nitrogen at room temperature for 2 h. The solvent was removed under vacuo, and the resulting oily residue was co-evaporated with toluene twice (2 × 10 mL), adsorbed on silica gel and applied to FC (silica gel, column 8 × 5 cm, CH_2Cl_2→CH_2Cl_2–MeOH, 95 : 5). Evaporation of the main fraction afforded **4f** (0.175 mg, 76%) as yellow solid. TLC (CH_2Cl_2–MeOH, 90 : 10) R_f 0.6. λ_{max} (MeOH)/nm 248 (ε/dm^3 mol^{-1} cm^{-1} 21 000), 255 (21 500), 260 (19 800), 276 (21 500). ^{1}H NMR (DMSO-d_6, 300 MHz) δ 1.06 (s, 21H, 3 × CH$(CH_3)_2$), 2.25–2.32 (m, 1H, H_α-2′), 3.49–3.59 (m, 2H, 2× H-5′), 3.83–3.87 (m, 1H, H-4′), 4.34–4.36 (m, 1H, H-3′), 4.97 (t, J = 5.4 Hz, 1H, HO-5′), 5.33 (d, J = 4.2 Hz, 1H, HO-3′), 6.45 (t, J = 6.5 Hz, 1H, H-1′), 7.92 (d, J = 9.0 Hz, 1H, H-7), 8.11 (dd, J = 2.3 Hz, 9.3 Hz, 1H, H-2), 8.26 (s, 1H, H-6), 8.37 (d, J = 2.1 Hz, 1H, H-4). ^{13}C NMR (DMSO-d_6, 75 MHz) δ 10.7, 18.5, 61.4, 70.4, 85.3, 87.7, 93.3, 98.8, 99.7, 112.1, 115.2, 118.1, 128.7, 133.1, 137.8, 142.0. ESI-TOF m/z calcd for $C_{24}H_{34}N_2O_5Si$ [M + Na]$^+$ 481.2129, found 481.2134.

1-(2-Deoxy-5-*O*-(4,4′-dimethoxytrityl)-β-D-*erythro*-pentofuranosyl)-3-[(triisopropylsilyl)-ethynyl]-5-nitroindole (9f). Compound **4f** (0.200 g, 0.44 mmol) was co-evaporated with pyridine (3 × 5 mL), then dissolved in pyridine (3 mL). Then, 4,4′-Dimethoxytritylchloride (0.190 g, 0.56 mmol) was added. The reaction mixture was stirred for 4 h at rt, CH_2Cl_2 (25 mL) was added and the solution was poured into a 5% $NaHCO_3$ solution (30 mL). The aq. layer was extracted with dichloromethane (30 mL), the combined organic layers were washed with brine, dried (Na_2SO_4), filtered and the solvent was evaporated. The resulting oil was co-evaporated with toluene (3 × 10 mL) and acetone (1 × 10 mL) furnishing a yellow foam which was applied to FC (silica gel, column 8 × 5 cm, CH_2Cl_2→CH_2Cl_2–acetone, 100 : 1). Evaporation of the main fraction afforded **9f** as light yellow foam (0.240 g, 72%). TLC (CH_2Cl_2–acetone, 95 : 5) R_f 0.5. λ_{max} (MeOH)/nm 236 (ε/dm^3 mol^{-1} cm^{-1} 38 900), 276 (26 100). ^{1}H NMR (DMSO-d_6, 300 MHz) δ 1.06 (s, 21H, TIPS), 2.34–2.43 (m, 1H, H_α-2′), 2.66–2.73 (m, 1H, H_β-2′), 3.11–3.12 (m, 2H, 2× H-5′), 3.67, 3.68 (2s, 6H, 2 × OCH_3), 3.95–3.99 (m, 1H, H-4′), 4.44 (m, 1H, H-3′), 5.38 (d, J = 3.3 Hz, 1H, HO-3′), 6.47 (t, J = 6.0 Hz, 1H, H-1′), 6.73–6.78 (m, 4H, Ar–H), 7.11–7.28 (m, 9H, Ar–H), 7.95 (d, J = 9.0 Hz, 1H, H-7), 8.08 (dd, J = 2.4 Hz, 9.0 Hz, 1H, H-2), 8.18 (s, 1H, H-6), 8.38 (d, J = 2.4 Hz, 1H, H-4). ^{13}C NMR (DMSO-d_6, 75 MHz) δ 10.6, 18.4, 54.8, 63.4, 70.0, 85.2, 85.3, 85.6, 93.3, 98.6, 99.5, 112.4, 112.9, 115.1, 118.0, 126.3, 127.4, 127.6, 128.7, 129.4, 129.7, 132.7, 135.0, 135.4, 137.8, 141.9, 144.7, 157.8, 157.9. ESI-TOF m/z calcd for $C_{45}H_{52}N_2O_7Si$ [M + Na]$^+$ 783.3436, found 783.3411.

1-(2-Deoxy-5-*O*-(4,4′-dimethoxytrityl)-β-D-*erythro*-pentofuranosyl)-3-[(triisopropylsilyl)-ethynyl]-5-nitroindole 3′-[(2-cyanoethyl)-(*N*,*N*-diisopropyl)]-phosphoramidite (10f). Compound **9f** (0.180 g, 0.23 mmol) was dissolved in anhydrous CH_2Cl_2 (5 mL). The mixture was treated with *N*,*N*-diisopropylethylamine (60 μL, 0.37 mmol) and 2-cyanoethyl diisopropylphosphoramidochloridite (75 μL, 0.33 mmol) for 30 min at rt. The solution was diluted with CH_2Cl_2 (20 mL) and poured into a 5% $NaHCO_3$ solution (30 mL). The aqueous layer was extracted with CH_2Cl_2 (3 × 30 mL), the combined organic layers were dried (Na_2SO_4), filtrated and evaporated. The residual foam was purified by FC (silica gel, column 8 × 5 cm, CH_2Cl_2→CH_2Cl_2–acetone, 80 : 1). Evaporation of the main fraction afforded **10f** (0.110 g, 48%) as yellow foam. TLC (CH_2Cl_2–acetone, 40 : 1) R_f 0.6. ^{31}P NMR ($CDCl_3$, 121.5 MHz) δ 148.8. ESI-TOF m/z calcd for $C_{54}H_{69}N_4O_8Psi$ [M + Na]$^+$ 983.4514, found 983.4482.

1-(2-Deoxy-β-D-*erythro*-pentofuranosyl)-3-[1-(pyrenmethyl)-1*H*-1,2,3-triazol-4-yl]-5-nitroindole (12). To a solution of **4d** (0.09 g, 0.30 mmol) and 1-azidomethylpyrene[16] (0.107 g, 0.42 mmol) in THF–H_2O–*t*-BuOH (3 : 1 : 1, 4 mL), sodium ascorbate (0.30 mL, 0.30 mmol) of a freshly prepared 1 M solution in water and copper(II) sulphate pentahydrate 7.5% in water (0.25 mL, 0.25 mmol) were added. The reaction mixture was stirred vigorously in the dark at room temperature and was monitored by TLC. After completion of the reaction, the

solvent was evaporated, and the residue was purified by FC (silica gel, column 10 cm × 3 cm, CH_2Cl_2–MeOH, 96 : 4) to give **12** as a yellow solid (0.110 g, 66%). TLC (CH_2Cl_2–MeOH, 90 : 10) R_f 0.55. λ_{max} (MeOH)/nm 260 (ε/dm^3 mol^{-1} cm^{-1} 30 400), 264 (42 300), 275 (64 000), 312 (18 900), 326 (36 200), 342 (49 200). ^{1}H NMR (DMSO-d_6, 300 MHz) δ 2.30 (br s, 1H, H_α-2′), 2.50 (br s, 1H, H_β-2′), 3.49 (m, 2H, 2× H-5′), 3.83 (br s, 1H, H-4′), 4.34 (br s, 1H, H-3′), 4.87 (t, J = 5.4 Hz, 1H, HO-5′), 5.32 (d, J = 3.0 Hz, 1H, HO-3′), 6.45–6.48 (m, 3H, H-1′, N–CH_2), 7.85 (d, J = 9.3 Hz, 1H, Ar–H), 8.07–8.57 (m, 12H, Ar–H), 9.12 (s, 1H, Ar–H). ^{13}C NMR (DMSO-d_6, 75 MHz) δ 51.1, 61.6, 70.5, 84.7, 87.4, 109.2, 111.3, 117.4, 117.7, 120.7, 122.7, 123.7, 124.1, 124.9, 125.1, 125.6, 125.7, 126.3, 126.5, 127.2, 127.7, 127.8, 128.4, 128.5, 128.9, 130.1, 130.7, 131.1, 138.9, 141.4, 141.6. ESI-TOF m/z calculated for $C_{32}H_{25}N_5O_5$ $[M + Na]^+$ 582.1748, found 582.1746.

1-(2-Deoxy-β-D-*erythro*-pentofuranosyl)-3-[6-{1-(pyren-1-ylmethyl)-1*H*-1,2,3-triazol-4-yl}hex-1-yn-1-yl]-5-nitroindole (13). To a solution of **4e** (0.09 g, 0.24 mmol) and 1-azidomethylpyrene (0.085 g, 0.33 mmol) in THF–H_2O–*t*-BuOH (3 : 1 : 1, 4 mL), sodium ascorbate (0.24 mL, 0.24 mmol) of a freshly prepared 1 M solution in water and copper(II) sulphate pentahydrate 7.5% in water (0.20 mL, 0.06 mmol) were added. The reaction mixture was stirred vigorously in the dark at room temperature and was monitored by TLC. After completion of the reaction, the solvent was evaporated, and the residue was purified by FC (silica gel, column 10 cm × 3 cm, CH_2Cl_2–MeOH, 96 : 4) to give **13** as a yellow solid (0.108 g, 72%). TLC (CH_2Cl_2–MeOH, 90 : 10) R_f 0.56. λ_{max} (MeOH)/nm 260 (ε/dm^3 mol^{-1} cm^{-1} 27 600), 264 (39 700), 275 (65 100), 312 (20 200), 326 (35 500), 342 (45 900). ^{1}H NMR (DMSO-d_6, 300 MHz) δ 1.59–1.74 (m, 4H, 2 × CH_2), 2.31–2.50 (m, 4H, CH_2, H_α-2′, H_β-2′), 2.65 (br s, 2H, CH_2), 3.54 (br s, 2H, H-5′), 3.86 (br s, 1H, H-4′), 4.37 (br s, 1H, H-3′), 4.98 (t, J = 5.4 Hz, 1H, HO-5′), 5.35 (br s, 1H, HO-3′), 6.31 (s, 2H, CH_2), 6.44 (t, J = 6.0 Hz, 1H, CH_2), 7.84–8.51 (m, 14H, Ar–H). ^{13}C NMR (DMSO-d_6, 75 MHz) δ 18.5, 24.3, 27.7, 28.1, 50.6, 61.4, 70.4, 71.8, 85.0, 87.5, 93.3, 100.3, 111.6, 115.4, 117.7, 122.0, 122.6, 123.6, 123.9, 124.9, 125.4, 125.5, 126.3, 127.1, 127.3, 127.6, 128.1, 128.2, 129.2, 130.0, 130.6, 130.8, 131.8, 137.6, 141.5, 146.8. ESI-TOF m/z calculated for $C_{38}H_{33}N_5O_5$ $[M + Na]^+$ 662.2374, found 662.2356.

3-Acetyl-1-(2-deoxy-β-D-*erythro*-pentofuranosyl)-5-nitroindole (16). To a solution of compound **4d** (0.060 g, 0.20 mmol) in MeOH (9 mL) was added water (1 mL) and H_2SO_4 (0.02 mmol). The reaction mixture was stirred for 6 h at 75 °C. The reaction mixture was neutralized with aq. NH_3 and evaporated to dryness. The remaining residue was purified by FC (silica gel, column 10 × 2 cm, CH_2Cl_2–MeOH, 90 : 10) to give the product **16** (0.050 g, 78%) as a colorless powder. TLC (CH_2Cl_2–MeOH, 90 : 10) R_f 0.63. λ_{max} (MeOH)/nm 260 (ε/dm^3 mol^{-1} cm^{-1} 27 700), 267 (28 500) 313, (9100). ^{1}H NMR (DMSO-d_6, 300 MHz) δ 2.33–2.40 (m, 1H, H_α-2′), 2.50 (s, 3H, CH_3), 2.53–2.62 (m, 1H, H_β-2′), 3.53–3.65 (m, 2H, 2× H-5′), 3.89–3.90 (m, 1H, H-4′), 4.41 (br s, 1H, H-3′), 5.06 (t, J = 4.8 Hz, 1H, HO-5′), 5.37 (d, J = 3.6 Hz, 1H, HO-3′), 6.48 (d, J = 6.3 Hz, 1H, H-1′), 7.92 (d, J = 9.3 Hz, 1H, Ar–H), 8.16 (dd, J = 1.8 Hz, 36.0 Hz, 1H, Ar–H), 8.81 (s, 1H, Ar–H), 9.01 (d, J = 1.8 Hz, 1H, Ar–H). ^{13}C NMR (DMSO-d_6, 75 MHz) δ 27.1, 60.9, 69.9, 85.4, 87.5, 111.9, 117.5, 118.1, 125.1, 136.8, 138.8, 142.8. ESI-TOF m/z calcd for $C_{15}H_{16}N_2O_6$ $[M + Na]^+$ 343.0901, found 343.0901.

Copper(I)-catalyzed [3 + 2] cycloaddition of alkynyl modified oligonucleotides with 1-azidomethylpyrene

To a solution of the ss-oligonucleotides **17** or **19** (3 A_{260} units, 30 μM) in 20 μL of water were added a mixture of the $CuSO_4$·TBTA (1 : 1) ligand complex (30 μL of a 20 mM stock solution in H_2O–DMSO–*t*-BuOH, 4 : 3 : 1), tris-(2-carboxyethyl)-phosphine (TCEP, 30 μL of a 20 mM stock solution in water), $NaHCO_3$ (30 μL, 200 mM stock solution in water), 1-azidomethylpyrene (**11**) (30 μL of a 20 mM stock solution in H_2O–dioxane–DMSO, 3 : 3 : 4), and DMSO (30 μL), and the reaction mixture was stirred at room temperature for 12 h. The reaction mixture was concentrated in a SpeedVac evaporator, and the residue was dissolved in 200 μL of bidistilled water and centrifuged for 20 min at 14 000 rpm. The supernatant was collected and further purified by reversed-phase HPLC with the gradient [A: MeCN; B: 0.1 M (Et_3NH)OAc (pH 7.0)–MeCN 95 : 5; gradient I: 0–3 min 10–15% A in B, 3–15 min 15–50% A in B, flow rate 0.8 cm^3 min^{-1}] to give the oligonucleotide pyrene conjugates in about 50% isolated yield. The molecular masses of the oligonucleotides were determined by MALDI-TOF mass spectra (Table S3†). Typical HPLC profiles of the oligonucleotides are shown in the ESI (Fig. S1†).

Tandem enzymatic hydrolysis of oligonucleotides

The enzymatic hydrolysis of ODN-**15** was performed using snake-venom phosphodiesterase (EC 3.1.15.1, *Crotallus adamanteus*) and alkaline phosphatase (EC 3.1.3.1, *Escherichia coli*) in 0.1 M Tris-HCl buffer (pH 8.5) at 37 °C. The enzymatic digestion products were analyzed by reversed-phase HPLC using the following gradients: gradient III: 0–20 min 100% B, 20–50 min 0–60% A in B; 50–55 min 60% A in B; flow rate 0.7 mL min^{-1} (A, MeCN; B 0.1 M (Et_3NH)OAc (pH 7.0)–MeCN, 95 : 5).

Deprotection of the TIPS group

Triisoproylsilylethynyl-modified ODN-**28** (10 A_{260} unit) was dissolved in CH_3CN–DMF (4 : 1, 150 μL) and tetrabutylammonium fluoride (10 μL). The resulting reaction mixture was stirred at room temperature for 16 h. The deprotected oligonucleotide was precipitated by adding 3 M NaOAc buffer, pH 5.2 (20 μL), and 2-propanol (600 μL) and incubated at 0 °C for 24 h. After centrifugation at 14 000 rpm for 30 min, the solvent was decanted and the remaining residue was washed with 75% ethanol (150 μL). The resulting oligonucleotide was purified by reversed-phase HPLC using gradient II.

Acknowledgements

We thank Dr S. Budow-Busse for helpful discussions and support while preparing the manuscript. We also thank

Mr S. S. Pujari and Mr H. Mei for measuring the NMR spectra and Mr Nhat Quang Tran for the oligonucleotide syntheses. We thank Dr M. Letzel, Organisch-Chemisches Institut, Universität Münster, Münster, Germany, for the measurement of the MALDI spectra. Financial support by ChemBiotech, Münster, Germany, is highly appreciated.

References

1 (*a*) D. Loakes, *Nucleic Acids Res.*, 2001, **29**, 2437–2447; (*b*) E. Ohtsuka, S. Matsuki, M. Ikehara, Y. Takahashi and K. Matsubara, *J. Biol. Chem.*, 1985, **260**, 2605–2608; (*c*) S. P. Sau and P. J. Hrdlicka, *J. Org. Chem.*, 2012, **77**, 5–16.

2 (*a*) F. Seela and C. Mittelbach, *Nucleosides Nucleotides*, 1999, **18**, 425–441; (*b*) Y. Kawase, S. Iwai, H. Inoue, K. Miura and E. Ohtsuka, *Nucleic Acids Res.*, 1986, **14**, 7727–7736.

3 (*a*) R. Nichols, P. C. Andrews, P. Zhang and D. E. Bergstrom, *Nature*, 1994, **369**, 492–493; (*b*) D. E. Bergstrom, P. Zhang, P. H. Toma, P. C. Andrews and R. Nichols, *J. Am. Chem. Soc.*, 1995, **117**, 1201–1209; (*c*) F. Seela and H. Debelak, *Nucleic Acids Res.*, 2000, **28**, 3224–3232; (*d*) J. He and F. Seela, *Org. Biomol. Chem.*, 2003, **1**, 1873–1883.

4 (*a*) D. Loakes and D. M. Brown, *Nucleic Acids Res.*, 1994, **22**, 4039–4043; (*b*) P. M. Vallone and A. S. Benight, *Nucleic Acids Res.*, 1999, **27**, 3589–3596; (*c*) H. Challa, M. L. Styers and S. A. Woski, *Org. Lett.*, 1999, **1**, 1639–1641; (*d*) P. Leonard, X. Ming, A. M. Jawalekar, W. Thür, D. Heindl and F. Seela, *Collect. Symp. Ser.*, 2005, **7**, 429–431; (*e*) D. E. Bergstrom, P. Zhang and W. T. Johnson, *Nucleic Acids Res.*, 1997, **25**, 1935–1942.

5 (*a*) D. Loakes, D. M. Brown, S. Linde and F. Hill, *Nucleic Acids Res.*, 1995, **23**, 2361–2366; (*b*) F. H. Martin, M. M. Castro, F. Aboul-ela and I. Tinoco Jr., *Nucleic Acids Res.*, 1985, **13**, 8927–8938; (*c*) D. Heindl, F. Bergmann, H.-P. Josel, D. Kessler, G. Lampert and C. Weilke, Labelling Reagent, *U.S. Patent*, 7,759,470 B2, 2010; (*d*) D. Heindl, T. Fröhlich, H. Maerz and M. Seller, Labelling Reagent, *U.S. Patent*, 7,759,469 B2, 2010; (*e*) K. Too and D. Loakes, Universal Base Analogues and their Application to Biotechnology, in *Modified Nucleosides: In Biochemistry, Biotechnology and Medicine*, ed. P. Herdewijn, Wiley-VCH, Weinheim, Germany, 2008, pp. 277–303; (*f*) S. Ball, M. A. Reeve, P. S. Robinson, F. Hill, D. M. Brown and D. Loakes, *Nucleic Acids Res.*, 1998, **26**, 5225–5227; (*g*) M. N. Preobrazhenskaya and I. A. Korbukh, The Synthesis and Reactions of Pyrrole, Pyrazole, Thiazole, Indole, Indazole, and Benzotriazole Nucleosides and Nucleotides, in *Chemistry of Nucleosides and Nucleotides*, ed. L. B. Townsend, Plenum press, New York, 1994, vol. 3, pp. 1–105.

6 (*a*) I. Hirao, M. Kimoto and R. Yamashige, *Acc. Chem. Res.*, 2012, **45**, 2055–2065; (*b*) D. A. Malyshev, K. Dhami, T. Lavergne, T. Chen, N. Dai, J. M. Foster, I. R. Corrêa Jr. and F. E. Romesberg, *Nature*, 2014, **509**, 385–388; (*c*) P. Marlière, J. Patrouix, V. Döring, P. Herdewijn, S. Tricot, S. Cruveiller, M. Bouzon and R. Mutzel, *Angew. Chem., Int. Ed.*, 2011, **50**, 7109–7114; (*d*) F. Liang, Y.-Z. Liu and P. Zhang, *RSC Adv.*, 2013, **3**, 14910–14928.

7 (*a*) G. Gaubert and J. Wengel, *Tetrahedron Lett.*, 2004, **45**, 5629–5632; (*b*) C. Wanninger and H.-A. Wagenknecht, *Synlett*, 2006, 2051–2054; (*c*) K. Too, D. M. Brown, P. Holliger and D. Loakes, *Collect. Czech. Chem. Commun. Symp. Ser.*, 2006, **71**, 899–911; (*d*) J. Gallego and D. Loakes, *Nucleic Acids Res.*, 2007, **35**, 2904–2912; (*e*) D. Loakes, J. Gallego, V. B. Pinheiro, E. T. Kool and P. Holliger, *J. Am. Chem. Soc.*, 2009, **131**, 14827–14837; (*f*) J. Barbaric, C. Wanninger-Weiß and H.-A. Wagenknecht, *Eur. J. Org. Chem.*, 2009, 364–370.

8 (*a*) C. L. Smith, A. C. Simmonds, A. L. Hamilton, D. L. Martin, A. G. Lashford, D. Loakes, F. Hill and D. M. Brown, *Nucleosides Nucleotides*, 1998, **17**, 555–564; (*b*) D. A. Harki, J. D. Graci, J. P. Edathil, C. Castro, C. E. Cameron and B. R. Peterson, *ChemBioChem*, 2007, **8**, 1359–1362.

9 (*a*) M. Kotera, A.-G. Bourdat, E. Defrancq and J. Lhomme, *J. Am. Chem. Soc.*, 1998, **120**, 11810–11811; (*b*) C. Crey-Desbiolles, N. Berthet, M. Kotera and P. Dumy, *Nucleic Acids Res.*, 2005, **33**, 1532–1543; (*c*) M. Kotera, Y. Roupioz, E. Defrancq, A.-G. Bourdat, J. Garcia, C. Coulombeau and J. Lhomme, *Chem. – Eur. J.*, 2000, **6**, 4163–4169.

10 (*a*) R. Huisgen, G. Szeimies and L. Möbius, *Chem. Ber.*, 1967, **100**, 2494–2507; (*b*) C. W. Tornøe, C. Christensen and M. Meldal, *J. Org. Chem.*, 2002, **67**, 3057–3064; (*c*) V. V. Rostovtsev, L. G. Green, V. V. Fokin and K. B. Sharpless, *Angew. Chem., Int. Ed.*, 2002, **41**, 2596–2599; (*d*) P. Kele, G. Mezö, D. Achatz and O. S. Wolfbeis, *Angew. Chem., Int. Ed.*, 2009, **48**, 344–347; (*e*) H. Xiong and F. Seela, *J. Org. Chem.*, 2011, **76**, 5584–5597.

11 (*a*) F. Seela and X. Ming, *Helv. Chim. Acta*, 2008, **91**, 1181–1200; (*b*) X. Ming, P. Leonard, D. Heindl and F. Seela, *Nucleic Acids Symp. Ser.*, 2008, **52**, 471–472.

12 (*a*) L. Lista, A. Pezzella, A. Napolitano and M. d'Ischia, *Tetrahedron*, 2008, **64**, 234–239; (*b*) C. Mothes, S. Lavielle and P. Karoyan, *J. Org. Chem.*, 2008, **73**, 6706–6710.

13 E. A. Motea, I. Lee and A. J. Berdis, *Nucleic Acids Res.*, 2012, **40**, 2357–2367.

14 (*a*) F. Seela and W. Bourgeois, *Synthesis*, 1990, 945–950; (*b*) M. Hoffer, *Chem. Ber.*, 1960, **93**, 2777–2781.

15 S. Budow, P. Leonard, H. Eickmeier, H. Reuter and F. Seela, *Acta Crystallogr., Sect. C: Cryst. Struct. Commun.*, 2009, **65**, o100–o102.

16 S. Y. Park, J. H. Yoon, C. S. Hong, R. Souane, J. S. Kim, S. E. Matthews and J. Vicens, *J. Org. Chem.*, 2008, **73**, 8212–8218.

17 (*a*) M. S. Morales-Ríos, R. E. del Río and P. Joseph-Nathan, *Magn. Reson. Chem.*, 1989, **27**, 1039–1047; (*b*) M. S. Morales-Ríos, J. Espiñeira and P. Joseph-Nathan, *Magn. Reson. Chem.*, 1987, **25**, 377–395; (*c*) M. S. Morales-Ríos, P. Joseph-

Nathan, B. Wrackmeyer and E. Kupče, *Magn. Reson. Chem.*, 1993, **31**, 238–240; (*d*) G. Burton, A. A. Ghini and E. G. Gros, *Magn. Reson. Chem.*, 1986, **24**, 829–831.

18 S. A. Ingale, H. Mei, P. Leonard and F. Seela, *J. Org. Chem.*, 2013, **78**, 11271–11282.

19 (*a*) H. Mei, S. A. Ingale and F. Seela, *Tetrahedron*, 2013, **69**, 4731–4742; (*b*) S. A. Ingale and F. Seela, *Tetrahedron*, 2014, **70**, 380–391; (*c*) S. A. Ingale and F. Seela, *J. Org. Chem.*, 2013, **78**, 3394–3399; (*d*) F. Seela and V. R. Sirivolu, *Org. Biomol. Chem.*, 2008, **6**, 1674–1687.

20 (*a*) F. Seela and S. A. Ingale, *J. Org. Chem.*, 2010, **75**, 284–295; (*b*) S. A. Ingale, S. S. Pujari, V. R. Sirivolu, P. Ding, H. Xiong, H. Mei and F. Seela, *J. Org. Chem.*, 2012, **77**, 188–199.

21 (*a*) C. A. M. Seidel, A. Schulz and M. Sauer, *J. Phys. Chem.*, 1996, **100**, 5541–5553; (*b*) T. L. Netzel, *Tetrahedron*, 2007, **63**, 3491–3514; (*c*) H.-A. Wagenknecht, *Angew. Chem., Int. Ed.*, 2003, **42**, 2454–2460; (*d*) M. Manoharan, K. L. Tivel, M. Zhao, K. Nafisi and T. L. Netzel, *J. Phys. Chem.*, 1995, **99**, 17461–17472; (*e*) H.-A. Wagenknecht, *Nat. Prod. Rep.*, 2006, **23**, 973–1006; (*f*) F. Menacher, M. Rubner, S. Berndl and H.-A. Wagenknecht, *J. Org. Chem.*, 2008, **73**, 4263–4266; (*g*) C. Wanninger-Weiss, L. Valis and H.-A. Wagenknecht, *Bioorg. Med. Chem.*, 2008, **16**, 100–106; (*h*) K. Nakashima, S. Tanida, T. Miyamoto and S. Hashimoto, *J. Photochem. Photobiol., A*, 1998, **117**, 111–117.

22 F. Seela and A. M. Jawalekar, *Helv. Chim. Acta*, 2002, **85**, 1857–1868.

23 (*a*) U. B. Christensen and E. B. Pedersen, *Nucleic Acids Res.*, 2002, **30**, 4918–4925; (*b*) J. Telser, K. A. Cruickshank, L. E. Morrison, T. L. Netzel and C.-K. Chan, *J. Am. Chem. Soc.*, 1989, **111**, 7226–7232; (*c*) Y. Saito, Y. Miyauchi, A. Okamoto and I. Saito, *Chem. Commun.*, 2004, 1704–1705.

